Cell Host & Microbe
Article

Disparate Impact of Oxidative Host Defenses Determines the Fate of *Salmonella* during Systemic Infection in Mice

Neil A. Burton,[1,4] Nura Schürmann,[1,4] Olivier Casse,[1] Anne K. Steeb,[1] Beatrice Claudi,[1] Janine Zankl,[2] Alexander Schmidt,[3] and Dirk Bumann[1,*]
[1]Focal Area Infection Biology
[2]FACS Core Facility
[3]Proteomics Core Facility, Biozentrum
University of Basel, 4056 Basel, Switzerland
[4]These authors contributed equally to this work
*Correspondence: dirk.bumann@unibas.ch
http://dx.doi.org/10.1016/j.chom.2013.12.006

SUMMARY

Reactive oxygen and nitrogen species function in host defense via mechanisms that remain controversial. Pathogens might encounter varying levels of these species, but bulk measurements cannot resolve such heterogeneity. We used single-cell approaches to determine the impact of oxidative and nitrosative stresses on individual *Salmonella* during early infection in mouse spleen. *Salmonella* encounter and respond to both stresses, but the levels and impact vary widely. Neutrophils and inflammatory monocytes kill *Salmonella* by generating overwhelming oxidative stress through NADPH oxidase and myeloperoxidase. This controls *Salmonella* within inflammatory lesions but does not prevent their spread to more permissive resident red pulp macrophages, which generate only sublethal oxidative bursts. Regional host expression of inducible nitric oxide synthase exposes some *Salmonella* to nitrosative stress, triggering effective local *Salmonella* detoxification through nitric oxide denitrosylase. Thus, reactive oxygen and nitrogen species influence dramatically different outcomes of disparate *Salmonella*-host cell encounters, which together determine overall disease progression.

INTRODUCTION

Host defense against pathogens depends on generation of reactive oxygen species (ROS), using NADPH oxidase, and reactive nitrogen species (RNS), using inducible nitric oxide synthase (iNOS) (Fang, 2004; Nathan and Shiloh, 2000). ROS and RNS can inhibit or kill microbes, but it remains controversial if this is their main role in infection control (Fang, 2011; Horta et al., 2012; Hurst, 2012; Liu and Modlin, 2008; Slauch, 2011). Various pathogens are highly resistant to ROS and RNS stress due to protective mechanisms that directly interfere with NADPH oxidase or iNOS activities, detoxify ROS and RNS before these compounds can damage the pathogen, and/or repair or replace damaged pathogen components. Moreover, ROS and RNS have additional important functions as host signaling molecules that regulate a wide variety of innate immune mechanisms, including chemotaxis, signaling, cell activation, vasculature tension, etc., all of which could contribute to infection control.

Oxidative and nitrosative stresses have been extensively studied in various *Salmonella* infection models. In cell culture models, infected macrophages kill most *Salmonella* in the first few hours after uptake in a NADPH oxidase-dependent manner, whereas iNOS inhibits growth of surviving *Salmonella* from 5 hr after infection (Vazquez-Torres et al., 2000a). On the other hand, *Salmonella* can inhibit assembly of NADPH oxidase and intracellular targeting of iNOS, using its SPI-2 type III secretion system (Chakravortty et al., 2002; Vazquez-Torres et al., 2000b). In mouse models, NADPH oxidase is crucial for infection control similar to cell cultures (Mastroeni et al., 2000), but it is unclear if this is due to a direct bactericidal effect of ROS (Fang, 2011; Slauch, 2011). NADPH oxidase remains crucial for infection control over many days. However, it is unclear if *Salmonella* killing continues after the first few hours of infection (Grant et al., 2008). A recent report even suggested that ROS levels in vivo are generally too low to have a significant direct impact on wild-type *Salmonella* (Aussel et al., 2011). iNOS is dispensable for *Salmonella* control throughout the first 7 days of infection (Mastroeni et al., 2000; White et al., 2005) in spite of the substantial bacteriostatic effect of iNOS within a few hours after infection in cell culture infection models.

Most of these studies relied on in vitro cell culture infections or bulk analyses of infected tissues, but such approaches ignore the remarkable diversity of host cell types and microenvironments that are encountered by *Salmonella* during infection. It is possible that, in these complex host environments, *Salmonella* subsets are exposed to widely varying ROS and RNS levels that have differential impacts. Common bulk average measurements would miss this heterogeneity and thus might be difficult to interpret.

Here, we developed single-cell approaches to determine the impact of ROS and RNS on individual *Salmonella* in a mouse typhoid fever model. We focused on the first few days of acute

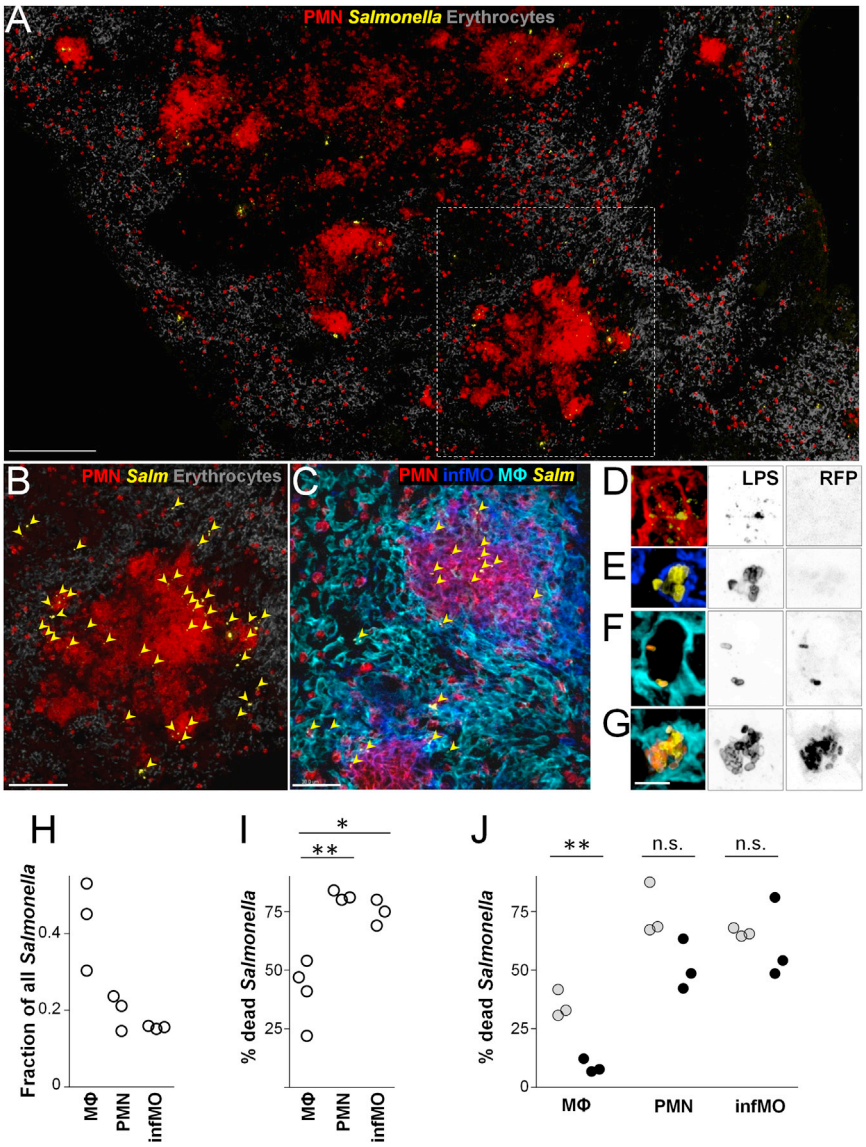

Figure 1. Disparate *Salmonella* Fates in Spleen Microenvironments

(A) Infected mouse spleen immunohistochemistry with markers for erythrocytes (Ter-119), polymorphonuclear neutrophils (PMNs; Ly-6G), and *Salmonella* (anti-lipopolysaccharide, LPS). The area labeled with a dashed line is shown at a higher magnification in (B). The scale bar represents 200 μm. Similar observations were made for 10 BALB/c mice and 10 C57BL/6 mice.

(B) Higher magnification of labeled area in (A). Yellow arrowheads indicate *Salmonella*. The scale bar represents 100 μm.

(C) Identification of infected neutrophils (PMN), inflammatory monocytes (infMO), resident red pulp macrophages (MΦ), and *Salmonella* (Salm) (Gr-1, red; anti-CD11b, blue; F4/80, cyan; anti-LPS, yellow; for use of infiltrate markers see Figure S1). The scale bar represents 30 μm.

(D–G) Live and dead *Salmonella* (yellow, anti-LPS; orange, RFP) in a neutrophil (D), an inflammatory monocyte (E), and two resident macrophages (F) (G). LPS and RFP channels are also shown as inverted grayscale images for better visibility of weak signals.

(H) Distribution of intracellular *Salmonella* among various host cell types. The data represent results from three BALB/c mice (total n of all *Salmonella*, 1,363).

(I) Proportions of dead *Salmonella* in various host cell types. The data represent results from three BALB/c mice (total n of all *Salmonella*, 619; **p = 0.0042; *p = 0.011; two-tailed t test).

(J) Proportions of dead *Salmonella* at day 4 after infection in mice that had received an isotype control antibody (gray) or anti-IFNγ (black) at day 3. Data from three BALB/c mice in each group are shown ($n_{control}$, 624; $n_{IFN\gamma}$, 436; **p = 0.0022). See also Figure S1.

infection. Our goal was to clarify controversial issues, including the extent of *Salmonella* killing by host defenses, the impact of ROS and RNS on *Salmonella* properties and fates, and the potential role of diverse *Salmonella*-host encounters on overall disease progression.

RESULTS

Oxidative Killing of *Salmonella* by Neutrophils and Monocytes in Inflammatory Lesions

To determine in which tissue microenvironments *Salmonella* reside during infection, we analyzed fixed spleen cryosections using immunohistochemistry. At day 4 after infection, *Salmonella* colonized spleen red pulp, but rarely the white pulp (Figures 1A and 1B), consistent with previous observations (Nix et al., 2007). Neutrophils and inflammatory monocytes accumulated in inflammatory lesions in infected regions, as expected (Richter-Dahlfors et al., 1997; Rydström and Wick, 2007). *Salmonella* resided in neutrophils and monocytes within lesions and primarily in resident red pulp macrophages outside of these lesions (Figures 1C–1H).

An antibody to *Salmonella* lipopolysaccharide (LPS) stains both live and dead *Salmonella*, but intracellular retention of fluorescent proteins discriminates live from dead *Salmonella* (Barat et al., 2012). Using *Salmonella* expressing the red fluorescent protein mCherry (RFP), we determined that most *Salmonella* within neutrophils and inflammatory monocytes in inflammatory lesions were dead (LPS^+ RFP^-; Figures 1D, 1E, and 1I). Large lesions contained little detectable LPS, suggesting successful *Salmonella* clearance. In comparison, red pulp macrophages outside of inflammatory lesions contained lower proportions of dead *Salmonella* (LPS^+ RFP^+; Figures 1F, 1G, and 1I). *Salmonella* killing in macrophages was almost abolished in mice treated with a neutralizing antibody to interferon gamma (IFNγ; Figure 1J), consistent with the crucial role of IFNγ in early *Salmonella* control (Gulig et al., 1997; Muotiala, 1992; VanCott et al., 1998) and activation of macrophage bactericidal activity (Vazquez-Torres et al., 2000a).

Cybb$^{-/-}$ mice deficient for cytochrome b-245 heavy chain, an essential subunit of NADPH oxidase, are hypersusceptible to

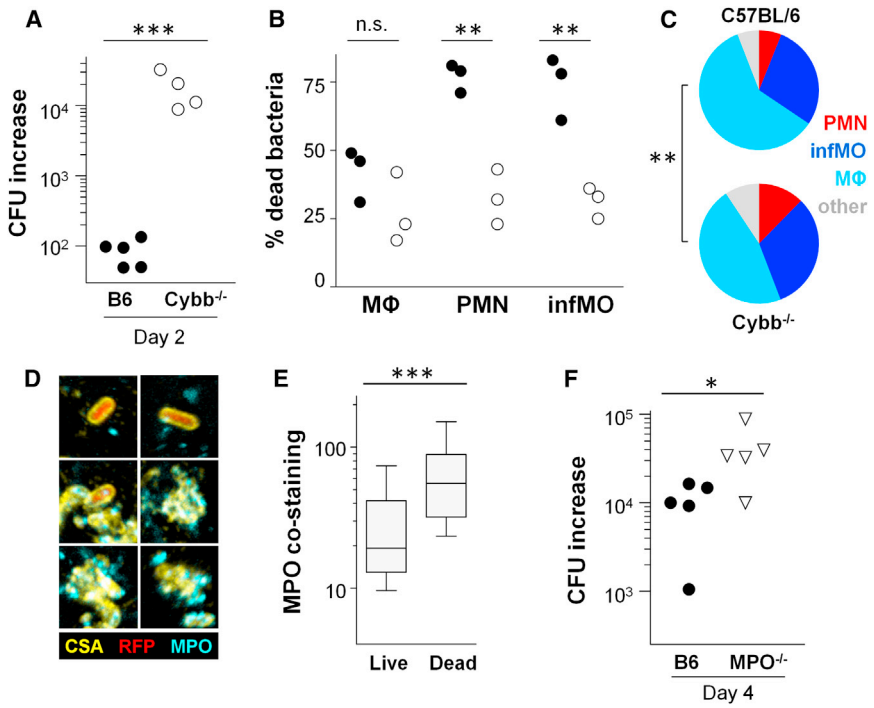

Figure 2. Neutrophils and Monocytes Kill *Salmonella* through Oxidative Stress

(A) *Salmonella* growth in C57BL/6 (B6) and congenic *Cybb*$^{-/-}$ mice. Data represent *Salmonella* spleen loads of individual mice at day 2 divided by the inoculum dose (***$p < 0.001$, two-tailed t test of log-transformed data).

(B) Proportion of live *Salmonella* in neutrophils (PMN), inflammatory monocytes (infMO), and resident macrophages (MΦ) in C57BL/6 (filled circles, n = 613) and Cybb$^{-/-}$ (open circles, n = 579) mice.

(C) Distribution of live *Salmonella* among different host cell types in C57BL/6 and *Cybb*$^{-/-}$ mice. The data represent averages from three mice (**p = 0.0032, two-way ANOVA).

(D) Colocalization of live and dead *Salmonella* with myeloperoxidase (yellow, common *Salmonella* antigen, CSA; red, RFP; cyan, MPO). Similar observations were made for three mice.

(E) Myeloperoxidase (MPO) concentrations around live and dead *Salmonella*. The data are represented as box plots (central line is the median; the box includes the central 50%; whiskers, 10^{th}–90^{th} percentile; ***$p < 0.001$; Mann-Whitney U test; total n = 159).

(F) *Salmonella* growth in C57BL/6 (B6) and congenic *MPO*$^{-/-}$ mice. Data represent *Salmonella* spleen loads of individual mice at day 4 divided by the inoculum dose (*p = 0.042, two-tailed t test of log-transformed data).

Salmonella infection (Mastroeni et al., 2000). The high spleen loads in such mice (Figure 2A) correlated with less *Salmonella* killing in neutrophils and inflammatory monocytes, whereas *Salmonella* live/dead ratios in resident macrophages remained unaltered (Figure 2B). As a consequence, higher proportions of live *Salmonella* resided in neutrophils and inflammatory monocytes in *Cybb*$^{-/-}$ mice (Figure 2C). These data indicated that neutrophils and inflammatory monocytes effectively killed *Salmonella* using NADPH oxidase, while resident macrophages used less effective, largely NADPH oxidase-independent *Salmonella* killing mechanisms.

NADPH oxidase generates superoxide $O_2^{\bullet-}$, which spontaneously dismutates to hydrogen peroxide H_2O_2 and molecular oxygen. Neutrophils and inflammatory monocytes, but not resident macrophages, express myeloperoxidase (MPO), which converts almost all $O_2^{\bullet-}$ or H_2O_2 into highly bactericidal hypohalites: hypochlorite OCl^- (bleach), hypobromite, and/or hypoiodite (Klebanoff et al., 2013; Swirski et al., 2010). Myeloperoxidase preferentially colocalized with dead *Salmonella* (Figures 2D and 2E), and *MPO*$^{-/-}$ mice deficient for myeloperoxidase had slightly elevated *Salmonella* loads (Figure 2F). Together, these data suggest a contribution of hypochlorite (and/or related species) in *Salmonella* killing.

Nevertheless, myeloperoxidase was largely dispensable for *Salmonella* control, indicating alternative NADPH oxidase-mediated killing mechanisms. In the absence of myeloperoxidase, neutrophils accumulate $O_2^{\bullet-}$ and H_2O_2 (Winterbourn et al., 2006). To explore their potential impact on *Salmonella*, we combined a published computational model for oxidative bursts in neutrophil phagosomes (Winterbourn et al., 2006) with in vivo expression data for *Salmonella* ROS defense enzymes (Steeb et al., 2013). This in silico model predicted superoxide and hydrogen peroxide accumulation in the phagosomal lumen in the absence of myeloperoxidase (Figure 3), as expected (Winterbourn et al., 2006). According to the model, superoxide was largely present in the deprotonated form of $O_2^{\bullet-}$ that poorly penetrates into bacteria (Korshunov and Imlay, 2002), whereas H_2O_2 reached levels around 15 μM within *Salmonella*, far above the lethality threshold for *Salmonella* (~2 μM; Seaver and Imlay, 2001). This was the consequence of phagosomal H_2O_2 (17 μM) readily diffusing through the *Salmonella* envelope (Seaver and Imlay, 2001) at rates matching the *Salmonella* detoxification rate (0.15×10^6 molecules/s). *Salmonella* killing by moderate, but stable, levels of luminal H_2O_2 was consistent with previous data for high lethality of continuous H_2O_2 exposure (Park et al., 2005).

Interestingly, increasing *Salmonella* detoxification by 0.15×10^6 molecules/s (thus doubling its rate) would marginally affect predicted phagosomal H_2O_2 (16.3 μM versus 17 μM), due to buffering by rapid H_2O_2 diffusion from the phagosome to the host cell cytosol (3.8×10^6 molecules/s; Figure 3). This diffusion is, by definition, proportional to the concentration gradient between phagosome and cytosol, and a slight decrease of phagosomal H_2O_2 from 17 μM to 16.3 μM would lower its rate by 0.15×10^6 s^{-1}. As *Salmonella* detoxification increased, less H_2O_2 would thus be lost to the host cell cytosol, and this compensated for the increase in *Salmonella* detoxification, resulting in almost unaltered phagosomal and *Salmonella* concentrations.

Together, these data suggested NADPH oxidase-dependent oxidative killing of *Salmonella* in neutrophils (and inflammatory monocytes) either by hypohalites or by overwhelming hydrogen peroxide if myeloperoxidase was absent. In addition to such

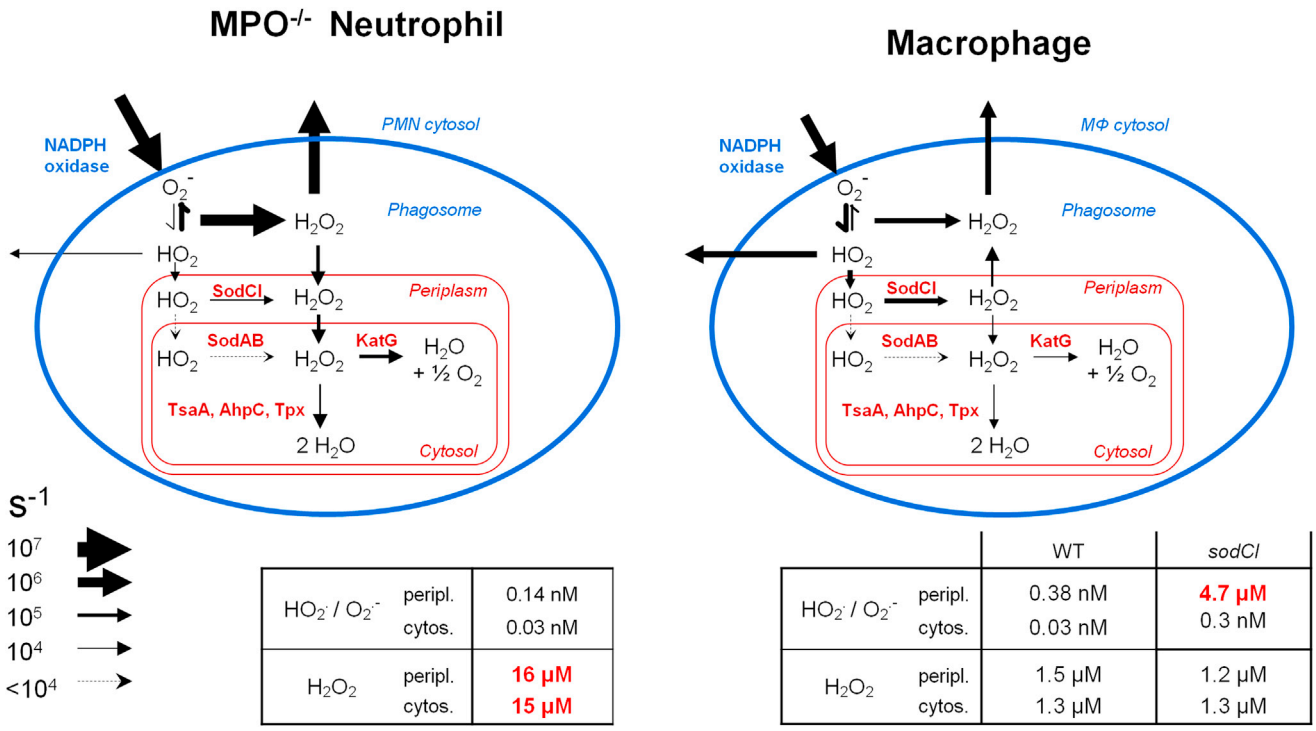

Figure 3. Computational Model of *Salmonella* Oxidative Stress in Phagosomes of Myeloperoxidase-Deficient Neutrophils and Wild-Type Macrophages

Salmonella membranes and detoxifying enzymes are shown in red. Predicted concentrations for superoxide and hydrogen peroxide in wild-type *Salmonella* in MPO-deficient neutrophils and wild-type (WT) *Salmonella* or the *sodCI* mutant inside macrophages are also shown.

direct bactericidal ROS effects, synergism with other bactericidal mechanisms, including antimicrobial peptides and hydrolases, might contribute to *Salmonella* killing.

Moderate Oxidative Bursts Fail to Kill *Salmonella*

While *Salmonella* in neutrophils and monocytes were largely killed through NADPH oxidase-dependent mechanisms, most live *Salmonella* resided in macrophages with apparently little impact of NADPH oxidase (Figure 2B). To determine if such live *Salmonella* experienced any oxidative stress, we used *Salmonella* carrying an episomal *katGp-gfpOVA* fusion as a ROS biosensor (Figure 4A). The *katGp* promoter is activated when the transcription factor OxyR reacts with H_2O_2 (Dubbs and Mongkolsuk, 2012). This promoter has low baseline activity and a large dynamic range compared to previously used *ahpCp* (Aussel et al., 2011) (Figure 4B). We used the unstable GFP variant GFP_OVA (Rollenhagen et al., 2004) to measure current promoter activities instead of integrating over many hours with stable GFP. We coexpressed RFP from the *sifBp* promoter with constitutive in vivo expression (Rollenhagen et al., 2004) to distinguish autofluorescent host cell fragments and dead RFP^- *Salmonella* from live RFP^+ *Salmonella* regardless of their GFP content (Figure 4C).

Biosensor *Salmonella* showed normal virulence in infected mice and stably maintained the episomal *katGp-gfpOVA* fusion (>99% plasmid maintenance at day 5 after infection). Proteome analysis of ex vivo purified biosensor *Salmonella* revealed unaltered expression of OxyR regulon members compared to *Salmonella* without episomal fusion (Figure S2A), indicating negligible OxyR titration by multicopy *katGp*.

Live RFP^+ biosensors had heterogeneous green fluorescence distributions, with large GFP^{dim} and small, but highly reproducible, GFP^{bright} subpopulations (Figure 4D). This reflected heterogeneous *katGp* activities, as *gfpOVA* fusions to unrelated promoters had unimodal GFP distributions (Figure S2B). GFP^{bright} *Salmonella* resided in various host cell types (Figure S2C) but were absent in $Cybb^{-/-}$ mice, indicating specific responses to ROS generated by host NADPH oxidase (Figure 4D). In contrast, myeloperoxidase-deficient $MPO^{-/-}$ mice contained a larger fraction of GFP^{bright} *Salmonella*, consistent with enhanced H_2O_2 levels and leakage in these mice (see above). GFP^{dim} biosensors had green fluorescence levels close to those of control *Salmonella* without GFP but maintained active *katGp-gfpOVA* fusions as demonstrated by ex vivo sorting followed by in vitro stimulation or reinjection into mice (Figure 4E). This suggested that their low in vivo GFP content reflected limited ROS exposure instead of plasmid loss or mutation. Together, these data indicated heterogeneous oxidative stress levels in live *Salmonella*.

Heterogeneous ROS exposure could reflect temporal dynamics of host cell oxidative bursts, with peak ROS generation early after bacterial contact followed by extended periods with little ROS generation (VanderVen et al., 2009). To test this hypothesis, we injected ex vivo sorted RFP^+ GFP^{dim} biosensor *Salmonella* into mice preinfected with nonfluorescent *Salmonella* (to ensure ongoing tissue inflammation). A large majority of

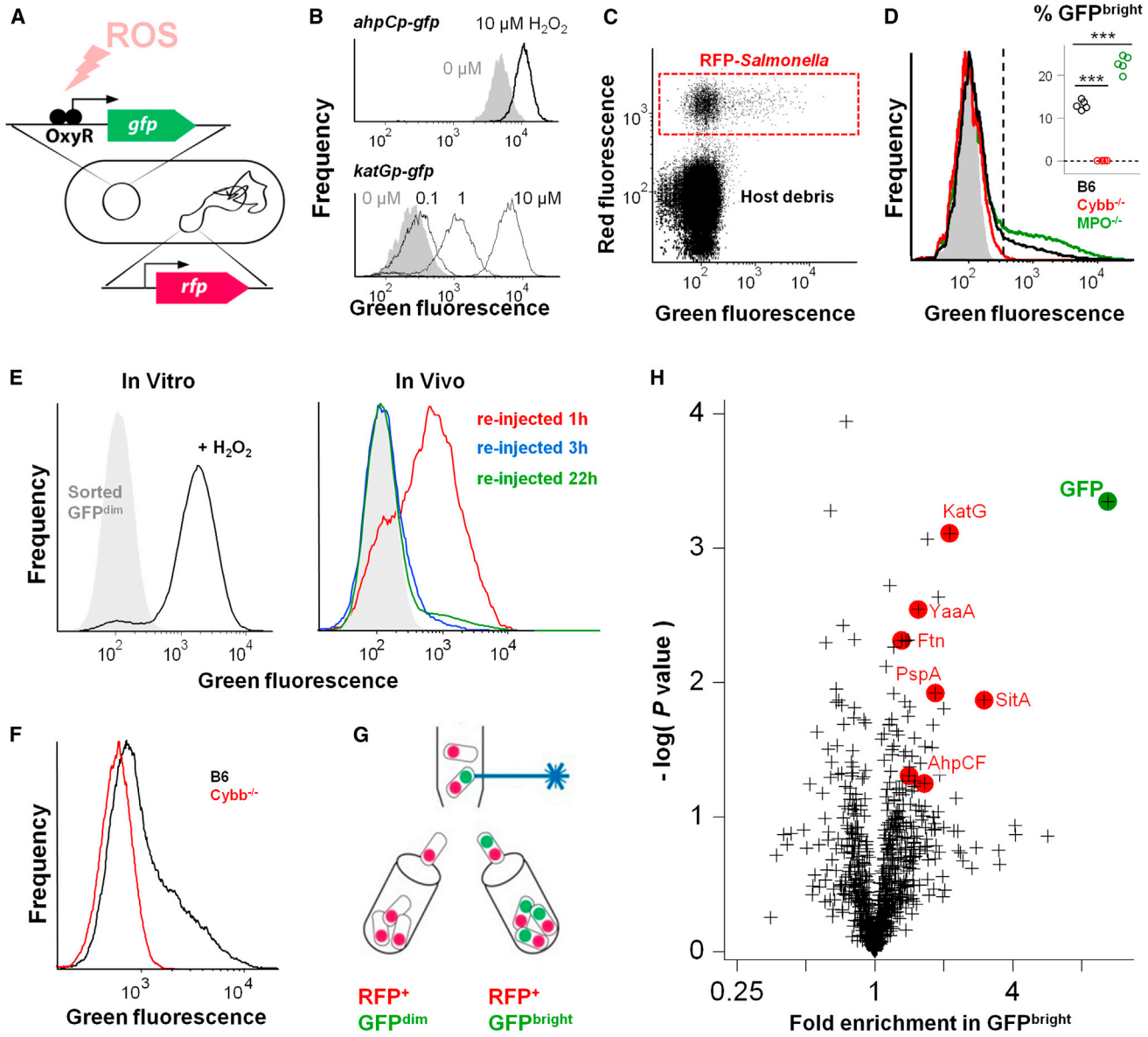

Figure 4. *Salmonella* Responses to Sublethal Oxidative Bursts

(A) ROS biosensor *Salmonella* expressing the GFP from an OxyR-activated promoter and the red fluorescent protein mCherry (RFP) from a constitutively active chromosomal promoter.

(B) In vitro responses of ROS biosensor *Salmonella* carrying different promoter-*gfp* fusions to H_2O_2 as determined by flow cytometry.

(C) Detection of RFP-expressing biosensor *Salmonella* in infected spleen homogenates using two-color flow cytometry.

(D) Green fluorescence intensities of ROS biosensor *Salmonella* in C57BL/6 (B6), *Cybb*$^{-/-}$, and *MPO*$^{-/-}$ mice. The shaded area corresponds to *Salmonella* without GFP. The inset shows the proportion of bright bacteria in individual mice (***$p < 0.001$, two-tailed t test).

(E) Restimulation of ex vivo isolated GFP^{dim} biosensor *Salmonella* (shaded gray area) in vitro (left) or in vivo at different times after reinjection into mice already infected with nonfluorescent *Salmonella* (right).

(F) Fluorescence intensities of ROS biosensor *Salmonella* expressing a stable GFP variant under control of the *katGp* promoter in C57BL/6 (B6) and *Cybb*$^{-/-}$ mice. Similar data were obtained for two mice of each line.

(G) Schematic representation of ex vivo purification of GFP^{bright} and GFP^{dim} biosensor *Salmonella* using flow cytometry.

(H) Proteome comparison of purified GFP^{bright} and GFP^{dim} ROS biosensor *Salmonella*. Data represent averages of independent samples purified from 3–4 BALB/c mice. Proteins labeled in red have been associated with ROS. See also Figure S2 and Table S1.

biosensor *Salmonella* activated *katGp* within 1 hr but became less active at 3 hr after injection (Figure 4E). At 20 hr after injection, we again observed the typical distribution with a small tail of GFP^{bright} *Salmonella*. We also constructed a modified *katGp-gfp* biosensor expressing stable GFP instead of unstable GFP_OVA. This modified biosensor showed larger proportions of NADPH oxidase-dependent GFP^{bright} *Salmonella* (Figure 4F) compared to the unstable GFP-biosensor, as expected for prolonged

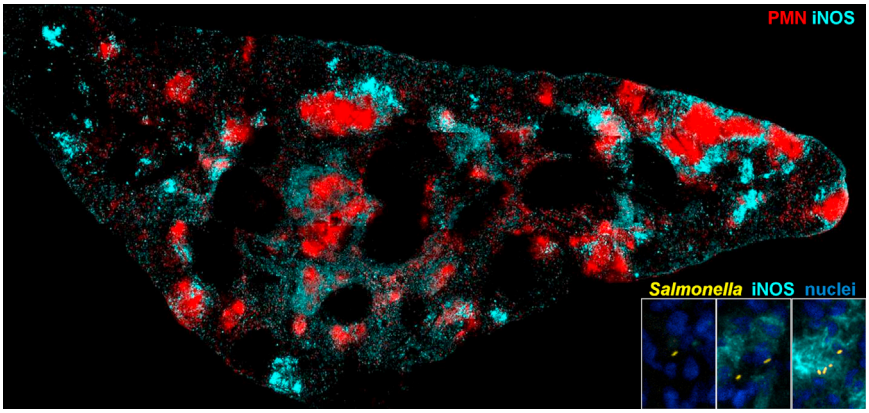

Figure 5. iNOS Expression in Infected Spleen

Infected mouse spleen immunohistochemistry with a marker for polymorphonuclear neutrophils (PMN, Ly-6G) and an antibody to inducible nitric oxide synthase (iNOS). The insets show higher magnifications (*Salmonella*, LPS; nuclei, DAPI). Similar observations were made for four BALB/c mice and four C57BL/6 mice.

GFP retention after transient expression. Together, these data were consistent with ROS exposures during transient host cell oxidative bursts. The small steady-state number of ROS biosensors with high *katGp* activities at later time points might reflect ongoing exposure of some *Salmonella* after spreading to new host cells.

To determine *Salmonella* responses to this transient ROS stress, we purified GFP^{dim} and GFP^{bright} subpopulations of *katGp-gfpOVA* biosensor *Salmonella* ex vivo (Figure 4G) and compared their proteomes. Abundance data for 966 different proteins revealed upregulation of several proteins involved in *Salmonella* oxidative stress defense, including catalase G and YaaA in GFP^{bright} biosensor *Salmonella* (Figure 4H, Table S1), supporting enhanced oxidative stress in this subpopulation. The protein profiles were otherwise highly similar, suggesting no major physiological differences between the two subpopulations. Interestingly, several *Salmonella* ROS defense proteins had very high abundance even in GFP^{dim} *Salmonella* (e.g., SodCI, 52,000 ± 2,000 copies per *Salmonella* cell; TsaA, 22,000 ± 2,000 copies; AhpC, 16,000 ± 2,000 copies). This could reflect residual low-level ROS exposure in this subset. Alternatively, *Salmonella* might stay prepared to cope with rapid onsets and short durations of host oxidative bursts (both within a few minutes), which cannot be efficiently countered by comparatively slow de novo protein synthesis.

Why were these oxidative bursts sublethal in resident red pulp macrophages? In part, this could reflect generally low NADPH oxidase activities in resident red pulp macrophages (Imlay, 2009; Nusrat et al., 1988). To explore this issue, we built a computational model of *Salmonella* oxidative stress in macrophage phagosomes based on our model for neutrophils (see above), but incorporating lower oxidative burst activities and acidic phagosomal pH (Figure 3). This in silico model predicted effective *Salmonella* ROS detoxification to sublethal concentrations in macrophages, in agreement with previous semiquantitative estimates (Imlay, 2009; Slauch, 2011). Interestingly, periplasmic SodCI was the only individual *Salmonella* defense enzyme with predicted critical impact on any ROS level. In the absence of SodCI, predicted $HO_2^{\bullet}$ concentration in the periplasm increased some 12,000-fold from 0.38 nM to 4.7 μM (Figure 3). Such high levels are likely to damage periplasmic biomolecules (Gort and Imlay, 1998). SodCI deficiency was also predicted to increase cytosolic $HO_2^{\bullet}$, but the resulting level (0.3 nM) was likely sublethal, given that external amino acids are available in vivo (Gort and Imlay, 1998; Steeb et al., 2013). These results are fully consistent with previous experimental data on the role of various *Salmonella* defense proteins (Craig and Slauch, 2009; De Groote et al., 1997; Uzzau et al., 2002).

Together, these data supported the hypothesis that NADPH oxidase activities in macrophages during early infection might be insufficient to overwhelm the potent and redundant *Salmonella* antioxidative defense. Our simplified computational model ignores potential synergism of ROS with RNS (Pacelli et al., 1995), antimicrobial peptides, hydrolases, and acidic conditions that might contribute to *Salmonella* killing. However, our data for *Cybb*$^{-/-}$ mice suggested that NADPH oxidase-mediated mechanisms were dispensable for *Salmonella* killing in resident macrophages (Figure 2B), arguing against a major role of direct bactericidal ROS, or synergism of ROS with other killing mechanisms, in these cells during early infection.

Local Nitrosative Stress Triggers Effective *Salmonella* Defense

In addition to ROS generation, *Salmonella*-infected tissues express iNOS (Khan et al., 2001; Umezawa et al., 1997). iNOS was predominantly expressed by inflammatory monocytes accumulating around an inner core of neutrophils in inflammatory lesions (Figure 5), as expected (Khan et al., 2001; Rydström and Wick, 2007; Umezawa et al., 1997). Live *Salmonella* resided both inside and outside of these regions, thus experiencing widely different iNOS concentrations (Figure 5 insets; Figure 6A).

To determine the impact of iNOS-generated RNS on local *Salmonella* populations, we used RFP^{+} *Salmonella* carrying an episomal *hmpAp-gfpOVA* fusion as an RNS biosensor (Figure 6B). *hmpAp* is repressed by active NsrR, but derepressed when NO inactivates NsrR (Bang et al., 2006; Tucker et al., 2008). As expected, this strain responded to stimulation with acidified nitrite. In infected mouse spleen, it stably maintained the episomal fusion (>99% plasmid maintenance at day 5 after infection) and showed normal virulence.

Live RFP^{+} biosensor *Salmonella* had bimodal green fluorescence distributions (Figure 6C) with large GFP^{bright} subpopulations in proportions that varied between individual mice (45% ± 15%). GFP^{bright} *Salmonella* were absent in iNOS-deficient mice, indicating specific biosensor responses to RNS generated by host iNOS, but not host endothelial NOS (eNOS) or endogenously produced *Salmonella* NO (Gilberthorpe and Poole, 2008). GFP^{dim} biosensors maintained active *hmpAp-gfpOVA* fusions as demonstrated by in vitro stimulation (Figure S3A)

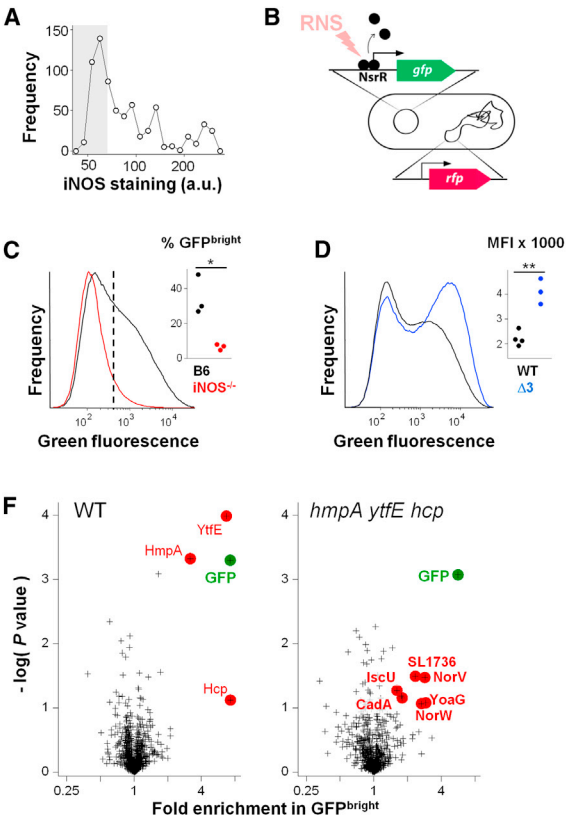

Figure 6. *Salmonella* Exposure and Responses to Nitrosative Stress

(A) Distribution of *Salmonella* among tissue regions with different iNOS concentrations. The shaded area represents background staining as observed for an *iNOS*$^{-/-}$ mouse.

(B) RNS biosensor *Salmonella* expressing the GFP from a NsrR-repressed promoter and the red fluorescent protein mCherry (RFP) from a constitutively active chromosomal promoter.

(C) Green fluorescence intensities of RNS biosensor *Salmonella* in C57BL/6 (B6) and *iNOS*$^{-/-}$ mice. The inset shows the proportion of bright bacteria in individual mice (*p = 0.013, two-tailed t test).

(D) Green fluorescence intensities of RNS biosensors in wild-type *Salmonella* (WT) and *Salmonella hmpA ytfE hcp* (Δ3). The inset shows the mean fluorescence intensities in individual mice (**p = 0.0016, two-tailed t test).

(E) iNOS concentrations around GFP^{dim} and GFP^{bright} RNS biosensor *Salmonella*. The data are represented as box plots (central line is the median; the box includes the central 50%; whiskers, 10th–90th percentile; ***p < 0.001; Mann-Whitney U test; total n = 690).

(F) Proteome comparison of purified GFP^{bright} and GFP^{dim} RNS biosensor in wild-type *Salmonella* (left) or *Salmonella hmpA ytfE hcp* (right). Data represent averages of independent samples from 3–4 BALB/c mice for each *Salmonella* strain. Proteins labeled in red have been associated with RNS. See also Figure S3 and Table S2.

and reinjection into mice (Figure S3B), suggesting that their initial low in vivo GFP content reflected limited RNS exposure instead of plasmid loss or mutation.

GFP^{bright} *Salmonella* resided in various phagocytes, including cells with low iNOS content, such as resident red pulp macrophages (Figure S2C). Many such GFP^{bright} *Salmonella*, however, had highly iNOS-positive cells in their close vicinity, likely reflecting the fact that NO can diffuse freely through cellular membranes (Pacher et al., 2007). Indeed, analysis of regional iNOS concentration within a radius of 15 μm (Leone et al., 1996) around individual *Salmonella* revealed a strong correlation between *Salmonella* GFP expression and local iNOS levels (Figure 6E).

RFP^{+} GFP^{bright} RNS biosensor *Salmonella* specifically upregulated three prototypical RNS defense proteins (Figure 6F; Table S2): HmpA, YtfE, and Hcp, which function as an NO denitrosylase (Hausladen et al., 2001), an iron sulfur cluster repair protein (Justino et al., 2007), and a hydroxylamine reductase (Wolfe et al., 2002), respectively. Hcp had low abundance around the detection threshold (100 ± 40 copies per *Salmonella* cell; detected in only 2 of 4 samples), resulting in poor statistical significance. All three proteins are subject to NsrR repression and upregulated upon NO exposure in vitro and in cell culture infections (Gilberthorpe et al., 2007; Kim et al., 2003; Richardson et al., 2011; Tucker et al., 2008), consistent with RNS stress specifically in GFP^{bright} *Salmonella*. Comparison of protein levels to *Salmonella* without episomal *hmpA-gfpOVA* fusion demonstrated normal NsrR activity without detectable NsrR titration by multicopy *hmpAp* (Figure S3C). Apart from HmpA, YtfE, and Hcp, GFP^{bright} and GFP^{dim} RNS biosensor *Salmonella* had highly similar protein profiles, suggesting no major physiological differences. This specific *Salmonella* response to RNS differed from observations for *Mycobacterium tuberculosis* that encounters multiple different stresses in tissue areas with high iNOS expression (Tan et al., 2013).

A *Salmonella hmpA ytfE hcp* triple mutant lacking all three upregulated proteins showed enhanced GFP fluorescence (Figure 6D), suggesting exacerbated RNS stress, as expected in the absence of the major NO detoxifying enzyme HmpA (Gilberthorpe et al., 2007). This exacerbated stress induced upregulation of alternative RNS defense enzymes, including NorVW (Gardner et al., 2002; Mills et al., 2008) in GFP^{bright} *Salmonella hmpA ytfE hcp* (Figure 6F), but did not result in growth attenuation (Figure S3D). *Salmonella hmpA ytfE hcp hcr norVW yoaG yeaR SL1344_1208 SL1344_1736 nrfABCDEFG nfnB cadABC metQ* lacking a total of 22 genes involved in RNS defense and repair (Bang et al., 2006; Bower and Mulvey, 2006; Justino et al., 2007; Richardson et al., 2011; Spiro, 2006; Wolfe et al., 2002) had a slight virulence defect, which could be rescued by a functional *hmpA* allele (Figure S3D), suggesting toxic effects of physiological RNS levels only when diverse *Salmonella* defense systems were all dysfunctional.

RNS have a minor impact on early salmonellosis in genetically susceptible BALB/c and C57BL/6 mice, but may have more profound effects in resistant mice carrying functional *Slc11a1* (*NRAMP1*) alleles (Henard and Vázquez-Torres, 2011). To investigate this further, we infected genetically resistant 129/Sv mice that, compared to BALB/c mice, controlled *Salmonella* much

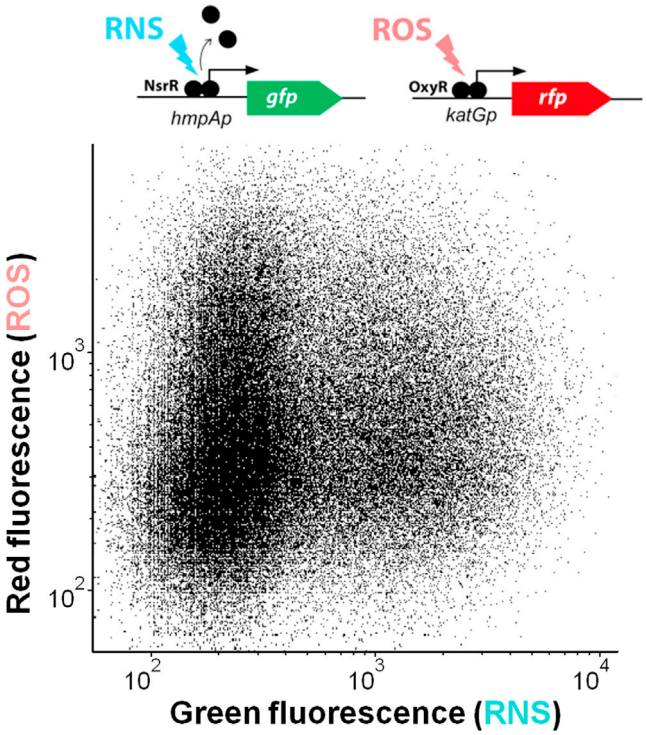

Figure 7. Exposure of Individual *Salmonella* to Oxidative and Nitrosative Stresses

Fluorescence intensities of dual RNS/ROS biosensor *Salmonella* expressing GFP from a NsrR-repressed promoter and the red fluorescent protein mCherry (RFP) from an OxyR-activated promoter in infected spleen. Similar observations were made for five mice. See also Figure S4.

better (Figure S3E), as expected. We observed patchy iNOS expression (Figure S3F) and heterogeneous *Salmonella hmpAp-gfpOVA* biosensor activities (Figure S3G) at day 5 and minor virulence defects of RNS defense mutants at day 8 (Figure S3H) in infected 129/Sv spleen, consistent with previous data for *Salmonella hmpA* at day 5 in a similar infection model (Bang et al., 2006), and no detectable role of iNOS for early *Salmonella* control in resistant mice (White et al., 2005).

Together, these data suggested similar heterogeneous sublethal RNS stresses for *Salmonella* during early infection in both susceptible and resistant mice. Future studies might investigate what mechanisms enable host RNS to effectively control *Salmonella* at later stages of infection (Bang et al., 2006; Mastroeni et al., 2000; White et al., 2005).

Lack of Coordination between Oxidative and Nitrosative Stresses

Salmonella biosensor data suggested ROS and RNS exposure of live *Salmonella* in similar host cell types (Figure S2C), raising the question as to whether these stresses co-occurred in the same cells. Comparison of proteome data revealed that ROS-induced proteins SitA, KatG, and YaaA were similarly abundant in *Salmonella* with high or low RNS exposure, whereas RNS-induced HmpA and YtfE were equally abundant in *Salmonella* regardless of ROS exposure (Figure S4), suggesting independently acting ROS and RNS stresses.

To further explore this issue, we constructed a dual ROS/RNS biosensor carrying ROS-responsive *katGp-rfp* and RNS-responsive *hmpAp-gfp* on compatible plasmids (and chromosomal *sifBp::cfp* as a constitutive marker for all live *Salmonella* cells). As expected, this biosensor responded in vitro to individual ROS or RNS stresses as well as to a ROS/RNS combination. In infected spleen, the dual biosensor stably maintained both plasmids and retained full virulence. Analysis of GFP and RFP expression in live CFP^+ biosensors revealed four distinct reproducible subpopulations (Figure 7): (i) 54% ± 3% GFP^{dim} RFP^{dim} *Salmonella* with low stress, (ii) 19% ± 1% GFP^{dim} RFP^{bright} *Salmonella* with substantial ROS but low RNS stress, (iii) 19% ± 1% GFP^{bright} RFP^{dim} *Salmonella* with substantial RNS but low ROS stress, and (iv) 9% ± 1% GFP^{bright} RFP^{bright}*Salmonella* exposed to both stresses (the proportion of ROS-stressed *Salmonella* appeared larger compared to *katGp-gfpOVA* data because we used stable RFP instead of unstable GFP as a reporter; the proportions of RNS-stressed *Salmonella* appeared lower compared to the single biosensor data because of differential plasmid copy numbers). *katGp-rfp* activities were similar among *Salmonella* with high or low RNS stress, and *hmpAp-gfp* activities were similar among *Salmonella* with high or low ROS stress (Figure 7). Together, these data confirmed largely independent action of ROS and RNS on *Salmonella*.

It is important to note that both approaches reported exclusively on live *Salmonella*, thus underestimating the proportion of *Salmonella* that were exposed to highly toxic ROS-RNS reaction products such as peroxynitrite. ROS/RNS synergy likely played a minor role in our conditions since iNOS has no detectable impact on early *Salmonella* control in susceptible mice (Henard and Vázquez-Torres, 2011), but it might become important at later stages when iNOS is involved in effective *Salmonella* control.

DISCUSSION

In this study, we used single-cell approaches to investigate key host defense mechanisms against *Salmonella* in a typhoid fever model. Our results show that many *Salmonella* experience and respond to ROS and RNS, but exposure levels and impact vary widely.

All three major infected host cell types (macrophages, neutrophils, inflammatory monocytes) can effectively kill *Salmonella* in vitro (Helaine et al., 2010; Rydström and Wick, 2009; Vazquez-Torres et al., 2000a), but in vivo evidence has been inconclusive (Benjamin et al., 1990; Broz et al., 2012; Grant et al., 2008; Gulig et al., 1997; Hormaeche, 1980; Lin et al., 1987; Miao et al., 2010). Our results showed extensive *Salmonella* killing, although this did not prevent continuous *Salmonella* net growth and disease progression. Neutrophils and inflammatory monocytes accumulated in inflammatory lesions around growing infection foci and efficiently killed *Salmonella*, but some *Salmonella* escaped to more permissive resident red pulp macrophages outside of inflammatory lesions. Our data were consistent with the strong, yet incomplete, control of salmonellosis by neutrophils and inflammatory monocytes (Conlan, 1997; Daley et al., 2008; Sheppard et al., 2003; Vassiloyanakopoulos et al., 1998) as well as *Salmonella*

tissue loads that increase primarily as a result of continuously forming new infection foci, while *Salmonella* growth inside existing infection foci is limited (Sheppard et al., 2003). The efficient control of local *Salmonella* growth within inflammatory lesions differed from the role of early granulomas in promoting mycobacterial proliferation during zebrafish tuberculosis (Ramakrishnan, 2012).

NADPH oxidase is essential for *Salmonella* control (Mastroeni et al., 2000), but the relevance of directly bactericidal ROS versus indirect effects was unclear (Fang, 2011; Hurst, 2012; Slauch, 2011). Our data suggested that neutrophils and inflammatory monocytes used NADPH oxidase and myeloperoxidase to kill *Salmonella* with bactericidal ROS. In contrast, resident macrophages imposed only sublethal, transient oxidative bursts on *Salmonella* during early infection and killed *Salmonella* through NADPH oxidase-independent mechanisms. Our data confirmed previously proposed nonlethal ROS levels (Aussel et al., 2011) for macrophages, but not neutrophils or monocytes. This partial agreement might reflect that previous studies compared live mutant and wild-type *Salmonella* (which mostly reside in macrophages) and did not account for lethal hypohalite action in neutrophils, thus focusing on readouts biased toward *Salmonella*-macrophage interactions.

Infected tissues expressed inducible nitric oxide synthase in some regions, which exposed local *Salmonella* to substantial RNS. However, these *Salmonella* upregulated defense proteins that provided full RNS protection in both susceptible and resistant mice during early infection. It is still unclear how host RNS can more effectively control *Salmonella* at later stages of infection.

Taken together, these data show how temporal and spatial ROS and RNS fluctuations generate at least six different *Salmonella* subpopulations with distinct properties and fates (live with low stress, live ROS stressed, live RNS stressed, live ROS/RNS stressed, killed by NADPH oxidase-dependent mechanisms, killed by unrelated mechanisms). Defects in host defense (as in *Cybb*$^{-/-}$, *MPO*$^{-/-}$, or *iNOS*$^{-/-}$ mice; IFNγ neutralization) or *Salmonella* stress protection (*hmpA ytfE hcp*) selectively affected only specific *Salmonella* subpopulations. Further studies might investigate why some *Salmonella* survive even in neutrophils and monocytes and how macrophages kill *Salmonella* through NADPH oxidase-independent mechanisms. Moreover, *Salmonella* experiences additional stresses, and both host and *Salmonella* activities show substantial cell-to-cell variation (Ackermann et al., 2008; Cummings et al., 2006; Diard et al., 2013; Dickinson et al., 2010; Li et al., 2009), suggesting that *Salmonella*-host interactions may be even more complex.

Overall, early mouse typhoid fever appears as a race between infiltrating host cells that accumulate around infection foci and kill local *Salmonella*, and *Salmonella* escaping to more permissive sites. The net balance of disparate *Salmonella*-host encounters with dramatically different individual outcomes thus determines overall disease progression. Similarly complex host-pathogen interactions might govern other infectious diseases, such as tuberculosis (Ramakrishnan, 2012; Tan et al., 2013; Yang et al., 2012). Single-cell in vivo approaches as used here might help to better understand this complexity and its impact on disease progression and control.

EXPERIMENTAL PROCEDURES

Bacterial Genetics

Salmonella strains (Table S3) were derived from *Salmonella enterica* serovar Typhimurium SL1344 (Hoiseth and Stocker, 1981). Promoter regions (see Supplemental Experimental Procedures) were cloned upstream of *gfp_ova*, *gfp*, or *mCherry* on pBR322- or pSC101-based plasmids. *Salmonella* mutants were generated using red recombinase-mediated allelic replacement followed by P22 phage transduction (Datsenko and Wanner, 2000).

Mouse Infections

All animal experiments were approved (license 2239, Kantonales Veterinäramt Basel-Stadt) and performed according to local guidelines (Tierschutz-Verordnung, Basel-Stadt) and the Swiss animal protection law (Tierschutz-Gesetz). Female mice (10–14 weeks old) were infected intravenously (i.v.) with *Salmonella* and euthanized 2–5 days later. Competitive indices of *Salmonella* mutants were determined by plating on selective media. Some mice received intraperitoneal (i.p.) injections with a neutralizing antibody to IFNγ. For detailed information on mouse strains and antibodies, see Supplemental Experimental Procedures.

Immunohistochemistry

Spleen portions were fixed with 4% paraformaldehyde, soaked in 40% sucrose, and frozen in optimal cutting temperature compound (OCT). Cryosections were stained with primary and secondary antibodies (see Supplemental Experimental Procedures) diluted in Tris-buffered saline (TBS)-Tween containing 2% mouse serum. Sections were mounted in 90% glycerol, 24.5 mg/ml DABCO, PBS (pH 7.4), and examined with Leica SP5 or Zeiss LSM 700 confocal microscopes (Biozentrum, Imaging Core Facility), using glycerol 20×, 40×, and 63× objectives. Image stacks were analyzed with Fiji and Imaris. We obtained high-resolution confocal stacks in which we could discriminate almost all individual *Salmonella* using envelope markers and RFP. In rare cases in which *Salmonella* could not be distinguished, clusters were counted as single *Salmonella*.

Flow Cytometry and Proteomics

Spleen was homogenized in ice-cold PBS containing 0.2% Triton X-100. All samples were kept on ice until analysis. Large host cell fragments were removed by centrifugation at 500 × *g* for 5 min. *Salmonella* were sedimented at 10,000 × *g* for 10 min and resuspended in PBS-Triton. Samples were analyzed in a Fortessa II Flow Cytometer, or sorted using a FACSAria III sorter. For specifications of optical channels, see Supplemental Experimental Procedures.

For proteome analysis, samples were prepared and sorted in PBS-Triton containing 170 μg/ml chloramphenicol to block de novo protein biosynthesis. Samples were digested with LysC and trypsin and analyzed by nanoscale liquid chromatography-tandem mass spectrometry (nLC-MS/MS). Peptides and proteins were identified by searching databases containing all predicted tryptic peptides for *Salmonella* SL1344 and mouse, as well as the corresponding decoy databases (Steeb et al., 2013). We only considered proteins with two identified peptides (at a 1% false discovery rate) that were detected in at least two independent samples.

Computational Modeling of *Salmonella* Oxidative Stress Protection

We build a diffusion-reaction model based on a previous neutrophil phagosome model (Winterbourn et al., 2006). We combined *Salmonella* dimensions and surface area with reported membrane permeabilities for various ROS. We derived *Salmonella* detoxification kinetics from experimental data on *Salmonella* protective enzyme expression as obtained by ex vivo proteomics (Steeb et al., 2013) and reported enzyme kinetic parameters (for parameters and equations, see Supplemental Experimental Procedures). Modeling was done using the Simulink feature of MATLAB.

SUPPLEMENTAL INFORMATION

Supplemental Information includes Supplemental Experimental Procedures, four figures, and three tables and can be found with this article online at http://dx.doi.org/10.1016/j.chom.2013.12.006.

AUTHOR CONTRIBUTIONS

D.B. conceived the study. D.B., N.A.B., N.S., and O.C. designed the experiments. All authors performed experiments and analyzed the data. O.C. wrote code and ran the models. D.B., N.A.B., and N.S. wrote the paper.

ACKNOWLEDGMENTS

We thank Mauricio Rosas Ballina for help with preparing figures, and the Swiss National Foundation (31003A-121834) and Deutsche Forschungsgemeinschaft (SPP1316 Bu971/6) for funding.

Received: August 6, 2013
Revised: October 25, 2013
Accepted: December 13, 2013
Published: January 15, 2014

REFERENCES

Ackermann, M., Stecher, B., Freed, N.E., Songhet, P., Hardt, W.D., and Doebeli, M. (2008). Self-destructive cooperation mediated by phenotypic noise. Nature *454*, 987–990.

Aussel, L., Zhao, W., Hébrard, M., Guilhon, A.A., Viala, J.P., Henri, S., Chasson, L., Gorvel, J.P., Barras, F., and Méresse, S. (2011). *Salmonella* detoxifying enzymes are sufficient to cope with the host oxidative burst. Mol. Microbiol. *80*, 628–640.

Bang, I.S., Liu, L., Vazquez-Torres, A., Crouch, M.L., Stamler, J.S., and Fang, F.C. (2006). Maintenance of nitric oxide and redox homeostasis by the *salmonella* flavohemoglobin hmp. J. Biol. Chem. *281*, 28039–28047.

Barat, S., Willer, Y., Rizos, K., Claudi, B., Mazé, A., Schemmer, A.K., Kirchhoff, D., Schmidt, A., Burton, N., and Bumann, D. (2012). Immunity to intracellular *Salmonella* depends on surface-associated antigens. PLoS Pathog. *8*, e1002966.

Benjamin, W.H., Jr., Hall, P., Roberts, S.J., and Briles, D.E. (1990). The primary effect of the *Ity* locus is on the rate of growth of *Salmonella typhimurium* that are relatively protected from killing. J. Immunol. *144*, 3143–3151.

Bower, J.M., and Mulvey, M.A. (2006). Polyamine-mediated resistance of uropathogenic *Escherichia coli* to nitrosative stress. J. Bacteriol. *188*, 928–933.

Broz, P., Ruby, T., Belhocine, K., Bouley, D.M., Kayagaki, N., Dixit, V.M., and Monack, D.M. (2012). Caspase-11 increases susceptibility to *Salmonella* infection in the absence of caspase-1. Nature *490*, 288–291.

Chakravortty, D., Hansen-Wester, I., and Hensel, M. (2002). *Salmonella* pathogenicity island 2 mediates protection of intracellular *Salmonella* from reactive nitrogen intermediates. J. Exp. Med. *195*, 1155–1166.

Conlan, J.W. (1997). Critical roles of neutrophils in host defense against experimental systemic infections of mice by *Listeria monocytogenes, Salmonella typhimurium*, and *Yersinia enterocolitica*. Infect. Immun. *65*, 630–635.

Craig, M., and Slauch, J.M. (2009). Phagocytic superoxide specifically damages an extracytoplasmic target to inhibit or kill *Salmonella*. PLoS ONE *4*, e4975.

Cummings, L.A., Wilkerson, W.D., Bergsbaken, T., and Cookson, B.T. (2006). In vivo, *fliC* expression by *Salmonella enterica* serovar Typhimurium is heterogeneous, regulated by ClpX, and anatomically restricted. Mol. Microbiol. *61*, 795–809.

Daley, J.M., Thomay, A.A., Connolly, M.D., Reichner, J.S., and Albina, J.E. (2008). Use of Ly6G-specific monoclonal antibody to deplete neutrophils in mice. J. Leukoc. Biol. *83*, 64–70.

Datsenko, K.A., and Wanner, B.L. (2000). One-step inactivation of chromosomal genes in *Escherichia coli* K-12 using PCR products. Proc. Natl. Acad. Sci. USA *97*, 6640–6645.

De Groote, M.A., Ochsner, U.A., Shiloh, M.U., Nathan, C., McCord, J.M., Dinauer, M.C., Libby, S.J., Vazquez-Torres, A., Xu, Y., and Fang, F.C. (1997). Periplasmic superoxide dismutase protects *Salmonella* from products of phagocyte NADPH-oxidase and nitric oxide synthase. Proc. Natl. Acad. Sci. USA *94*, 13997–14001.

Diard, M., Garcia, V., Maier, L., Remus-Emsermann, M.N., Regoes, R.R., Ackermann, M., and Hardt, W.D. (2013). Stabilization of cooperative virulence by the expression of an avirulent phenotype. Nature *494*, 353–356.

Dickinson, B.C., Huynh, C., and Chang, C.J. (2010). A palette of fluorescent probes with varying emission colors for imaging hydrogen peroxide signaling in living cells. J. Am. Chem. Soc. *132*, 5906–5915.

Dubbs, J.M., and Mongkolsuk, S. (2012). Peroxide-sensing transcriptional regulators in bacteria. J. Bacteriol. *194*, 5495–5503.

Fang, F.C. (2004). Antimicrobial reactive oxygen and nitrogen species: concepts and controversies. Nat. Rev. Microbiol. *2*, 820–832.

Fang, F.C. (2011). Antimicrobial actions of reactive oxygen species. MBio *2*, 00141–00111.

Gardner, A.M., Helmick, R.A., and Gardner, P.R. (2002). Flavorubredoxin, an inducible catalyst for nitric oxide reduction and detoxification in *Escherichia coli*. J. Biol. Chem. *277*, 8172–8177.

Gilberthorpe, N.J., and Poole, R.K. (2008). Nitric oxide homeostasis in *Salmonella typhimurium*: roles of respiratory nitrate reductase and flavohemoglobin. J. Biol. Chem. *283*, 11146–11154.

Gilberthorpe, N.J., Lee, M.E., Stevanin, T.M., Read, R.C., and Poole, R.K. (2007). NsrR: a key regulator circumventing *Salmonella enterica* serovar Typhimurium oxidative and nitrosative stress in vitro and in IFN-gamma-stimulated J774.2 macrophages. Microbiology *153*, 1756–1771.

Gort, A.S., and Imlay, J.A. (1998). Balance between endogenous superoxide stress and antioxidant defenses. J. Bacteriol. *180*, 1402–1410.

Grant, A.J., Restif, O., McKinley, T.J., Sheppard, M., Maskell, D.J., and Mastroeni, P. (2008). Modelling within-host spatiotemporal dynamics of invasive bacterial disease. PLoS Biol. *6*, e74.

Gulig, P.A., Doyle, T.J., Clare-Salzler, M.J., Maiese, R.L., and Matsui, H. (1997). Systemic infection of mice by wild-type but not Spv- *Salmonella typhimurium* is enhanced by neutralization of gamma interferon and tumor necrosis factor alpha. Infect. Immun. *65*, 5191–5197.

Hausladen, A., Gow, A., and Stamler, J.S. (2001). Flavohemoglobin denitrosylase catalyzes the reaction of a nitroxyl equivalent with molecular oxygen. Proc. Natl. Acad. Sci. USA *98*, 10108–10112.

Helaine, S., Thompson, J.A., Watson, K.G., Liu, M., Boyle, C., and Holden, D.W. (2010). Dynamics of intracellular bacterial replication at the single cell level. Proc. Natl. Acad. Sci. USA *107*, 3746–3751.

Henard, C.A., and Vázquez-Torres, A. (2011). Nitric oxide and salmonella pathogenesis. Front Microbiol *2*, 84.

Hoiseth, S.K., and Stocker, B.A. (1981). Aromatic-dependent *Salmonella typhimurium* are non-virulent and effective as live vaccines. Nature *291*, 238–239.

Hormaeche, C.E. (1980). The in vivo division and death rates of *Salmonella typhimurium* in the spleens of naturally resistant and susceptible mice measured by the superinfecting phage technique of Meynell. Immunology *41*, 973–979.

Horta, M.F., Mendes, B.P., Roma, E.H., Noronha, F.S., Macêdo, J.P., Oliveira, L.S., Duarte, M.M., and Vieira, L.Q. (2012). Reactive oxygen species and nitric oxide in cutaneous leishmaniasis. J. Parasitol. Res. *2012*, 203818.

Hurst, J.K. (2012). What really happens in the neutrophil phagosome? Free Radic. Biol. Med. *53*, 508–520.

Imlay, J.A. (2009). Oxidative Stress. In EcoSal, R.I.K, J.B. Curtiss, C.L. Squires, P.D. Karp, F.C. Neidhardt, and J.M. Slauch, eds. (Washington, DC: ASM Press).

Justino, M.C., Almeida, C.C., Teixeira, M., and Saraiva, L.M. (2007). *Escherichia coli* di-iron YtfE protein is necessary for the repair of stress-damaged iron-sulfur clusters. J. Biol. Chem. *282*, 10352–10359.

Khan, S.A., Strijbos, P.J., Everest, P., Moss, D., Stratford, R., Mastroeni, P., Allen, J., Servos, S., Charles, I.G., Dougan, G., and Maskell, D.J. (2001). Early responses to *Salmonella typhimurium* infection in mice occur at focal lesions in infected organs. Microb. Pathog. *30*, 29–38.

Kim, C.C., Monack, D., and Falkow, S. (2003). Modulation of virulence by two acidified nitrite-responsive loci of *Salmonella enterica* serovar Typhimurium. Infect. Immun. *71*, 3196–3205.

Klebanoff, S.J., Kettle, A.J., Rosen, H., Winterbourn, C.C., and Nauseef, W.M. (2013). Myeloperoxidase: a front-line defender against phagocytosed microorganisms. J. Leukoc. Biol. *93*, 185–198.

Korshunov, S.S., and Imlay, J.A. (2002). A potential role for periplasmic superoxide dismutase in blocking the penetration of external superoxide into the cytosol of Gram-negative bacteria. Mol. Microbiol. *43*, 95–106.

Leone, A.M., Furst, V.W., Foxwell, N.A., Cellek, S., and Moncada, S. (1996). Visualisation of nitric oxide generated by activated murine macrophages. Biochem. Biophys. Res. Commun. *221*, 37–41.

Li, X.J., Tian, W., Stull, N.D., Grinstein, S., Atkinson, S., and Dinauer, M.C. (2009). A fluorescently tagged C-terminal fragment of p47phox detects NADPH oxidase dynamics during phagocytosis. Mol. Biol. Cell *20*, 1520–1532.

Lin, F.R., Wang, X.M., Hsu, H.S., Mumaw, V.R., and Nakoneczna, I. (1987). Electron microscopic studies on the location of bacterial proliferation in the liver in murine salmonellosis. Br. J. Exp. Pathol. *68*, 539–550.

Liu, P.T., and Modlin, R.L. (2008). Human macrophage host defense against Mycobacterium tuberculosis. Curr. Opin. Immunol. *20*, 371–376.

Mastroeni, P., Vazquez-Torres, A., Fang, F.C., Xu, Y., Khan, S., Hormaeche, C.E., and Dougan, G. (2000). Antimicrobial actions of the NADPH phagocyte oxidase and inducible nitric oxide synthase in experimental salmonellosis. II. Effects on microbial proliferation and host survival in vivo. J. Exp. Med. *192*, 237–248.

Miao, E.A., Leaf, I.A., Treuting, P.M., Mao, D.P., Dors, M., Sarkar, A., Warren, S.E., Wewers, M.D., and Aderem, A. (2010). Caspase-1-induced pyroptosis is an innate immune effector mechanism against intracellular bacteria. Nat. Immunol. *11*, 1136–1142.

Mills, P.C., Rowley, G., Spiro, S., Hinton, J.C., and Richardson, D.J. (2008). A combination of cytochrome c nitrite reductase (NrfA) and flavorubredoxin (NorV) protects *Salmonella enterica* serovar Typhimurium against killing by NO in anoxic environments. Microbiology *154*, 1218–1228.

Muotiala, A. (1992). Anti-iFN-gamma-treated mice—a model for testing safety of live *Salmonella* vaccines. Vaccine *10*, 243–246.

Nathan, C., and Shiloh, M.U. (2000). Reactive oxygen and nitrogen intermediates in the relationship between mammalian hosts and microbial pathogens. Proc. Natl. Acad. Sci. USA *97*, 8841–8848.

Nix, R.N., Altschuler, S.E., Henson, P.M., and Detweiler, C.S. (2007). Hemophagocytic macrophages harbor *Salmonella enterica* during persistent infection. PLoS Pathog. *3*, e193.

Nusrat, A.R., Wright, S.D., Aderem, A.A., Steinman, R.M., and Cohn, Z.A. (1988). Properties of isolated red pulp macrophages from mouse spleen. J. Exp. Med. *168*, 1505–1510.

Pacelli, R., Wink, D.A., Cook, J.A., Krishna, M.C., DeGraff, W., Friedman, N., Tsokos, M., Samuni, A., and Mitchell, J.B. (1995). Nitric oxide potentiates hydrogen peroxide-induced killing of *Escherichia coli*. J. Exp. Med. *182*, 1469–1479.

Pacher, P., Beckman, J.S., and Liaudet, L. (2007). Nitric oxide and peroxynitrite in health and disease. Physiol. Rev. *87*, 315–424.

Park, S., You, X., and Imlay, J.A. (2005). Substantial DNA damage from submicromolar intracellular hydrogen peroxide detected in Hpx- mutants of *Escherichia coli*. Proc. Natl. Acad. Sci. USA *102*, 9317–9322.

Ramakrishnan, L. (2012). Revisiting the role of the granuloma in tuberculosis. Nat. Rev. Immunol. *12*, 352–366.

Richardson, A.R., Payne, E.C., Younger, N., Karlinsey, J.E., Thomas, V.C., Becker, L.A., Navarre, W.W., Castor, M.E., Libby, S.J., and Fang, F.C. (2011). Multiple targets of nitric oxide in the tricarboxylic acid cycle of *Salmonella enterica* serovar typhimurium. Cell Host Microbe *10*, 33–43.

Richter-Dahlfors, A., Buchan, A.M., and Finlay, B.B. (1997). Murine salmonellosis studied by confocal microscopy: *Salmonella typhimurium* resides intracellularly inside macrophages and exerts a cytotoxic effect on phagocytes in vivo. J. Exp. Med. *186*, 569–580.

Rollenhagen, C., Sörensen, M., Rizos, K., Hurvitz, R., and Bumann, D. (2004). Antigen selection based on expression levels during infection facilitates vaccine development for an intracellular pathogen. Proc. Natl. Acad. Sci. USA *101*, 8739–8744.

Rydström, A., and Wick, M.J. (2007). Monocyte recruitment, activation, and function in the gut-associated lymphoid tissue during oral *Salmonella* infection. J. Immunol. *178*, 5789–5801.

Rydström, A., and Wick, M.J. (2009). Monocyte and neutrophil recruitment during oral *Salmonella* infection is driven by MyD88-derived chemokines. Eur. J. Immunol. *39*, 3019–3030.

Seaver, L.C., and Imlay, J.A. (2001). Hydrogen peroxide fluxes and compartmentalization inside growing *Escherichia coli*. J. Bacteriol. *183*, 7182–7189.

Sheppard, M., Webb, C., Heath, F., Mallows, V., Emilianus, R., Maskell, D., and Mastroeni, P. (2003). Dynamics of bacterial growth and distribution within the liver during *Salmonella* infection. Cell. Microbiol. *5*, 593–600.

Slauch, J.M. (2011). How does the oxidative burst of macrophages kill bacteria? Still an open question. Mol. Microbiol. *80*, 580–583.

Spiro, S. (2006). Nitric oxide-sensing mechanisms in *Escherichia coli*. Biochem. Soc. Trans. *34*, 200–202.

Steeb, B., Claudi, B., Burton, N.A., Tienz, P., Schmidt, A., Farhan, H., Mazé, A., and Bumann, D. (2013). Parallel exploitation of diverse host nutrients enhances *Salmonella* virulence. PLoS Pathog. *9*, e1003301.

Swirski, F.K., Wildgruber, M., Ueno, T., Figueiredo, J.L., Panizzi, P., Iwamoto, Y., Zhang, E., Stone, J.R., Rodriguez, E., Chen, J.W., et al. (2010). Myeloperoxidase-rich Ly-6C+ myeloid cells infiltrate allografts and contribute to an imaging signature of organ rejection in mice. J. Clin. Invest. *120*, 2627–2634.

Tan, S., Sukumar, N., Abramovitch, R.B., Parish, T., and Russell, D.G. (2013). *Mycobacterium tuberculosis* responds to chloride and pH as synergistic cues to the immune status of its host cell. PLoS Pathog. *9*, e1003282.

Tucker, N.P., Hicks, M.G., Clarke, T.A., Crack, J.C., Chandra, G., Le Brun, N.E., Dixon, R., and Hutchings, M.I. (2008). The transcriptional repressor protein NsrR senses nitric oxide directly via a [2Fe-2S] cluster. PLoS ONE *3*, e3623.

Umezawa, K., Akaike, T., Fujii, S., Suga, M., Setoguchi, K., Ozawa, A., and Maeda, H. (1997). Induction of nitric oxide synthesis and xanthine oxidase and their roles in the antimicrobial mechanism against *Salmonella typhimurium* infection in mice. Infect. Immun. *65*, 2932–2940.

Uzzau, S., Bossi, L., and Figueroa-Bossi, N. (2002). Differential accumulation of *Salmonella*[Cu, Zn] superoxide dismutases SodCI and SodCII in intracellular bacteria: correlation with their relative contribution to pathogenicity. Mol. Microbiol. *46*, 147–156.

VanCott, J.L., Chatfield, S.N., Roberts, M., Hone, D.M., Hohmann, E.L., Pascual, D.W., Yamamoto, M., Kiyono, H., and McGhee, J.R. (1998). Regulation of host immune responses by modification of *Salmonella* virulence genes. Nat. Med. *4*, 1247–1252.

VanderVen, B.C., Yates, R.M., and Russell, D.G. (2009). Intraphagosomal measurement of the magnitude and duration of the oxidative burst. Traffic *10*, 372–378.

Vassiloyanakopoulos, A.P., Okamoto, S., and Fierer, J. (1998). The crucial role of polymorphonuclear leukocytes in resistance to *Salmonella dublin* infections in genetically susceptible and resistant mice. Proc. Natl. Acad. Sci. USA *95*, 7676–7681.

Vazquez-Torres, A., Jones-Carson, J., Mastroeni, P., Ischiropoulos, H., and Fang, F.C. (2000a). Antimicrobial actions of the NADPH phagocyte oxidase and inducible nitric oxide synthase in experimental salmonellosis. I. Effects on microbial killing by activated peritoneal macrophages in vitro. J. Exp. Med. *192*, 227–236.

Vazquez-Torres, A., Xu, Y., Jones-Carson, J., Holden, D.W., Lucia, S.M., Dinauer, M.C., Mastroeni, P., and Fang, F.C. (2000b). *Salmonella* pathogenicity island 2-dependent evasion of the phagocyte NADPH oxidase. Science *287*, 1655–1658.

White, J.K., Mastroeni, P., Popoff, J.F., Evans, C.A., and Blackwell, J.M. (2005). Slc11a1-mediated resistance to *Salmonella enterica* serovar

Typhimurium and *Leishmania donovani* infections does not require functional inducible nitric oxide synthase or phagocyte oxidase activity. J. Leukoc. Biol. *77*, 311–320.

Winterbourn, C.C., Hampton, M.B., Livesey, J.H., and Kettle, A.J. (2006). Modeling the reactions of superoxide and myeloperoxidase in the neutrophil phagosome: implications for microbial killing. J. Biol. Chem. *281*, 39860–39869.

Wolfe, M.T., Heo, J., Garavelli, J.S., and Ludden, P.W. (2002). Hydroxylamine reductase activity of the hybrid cluster protein from *Escherichia coli*. J. Bacteriol. *184*, 5898–5902.

Yang, C.T., Cambier, C.J., Davis, J.M., Hall, C.J., Crosier, P.S., and Ramakrishnan, L. (2012). Neutrophils exert protection in the early tuberculous granuloma by oxidative killing of mycobacteria phagocytosed from infected macrophages. Cell Host Microbe *12*, 301–312.